Electronic properties of monolayer steps on $(2\times4)/c(2\times8)$ reconstructed GaAs(001) surfaces

Kiyoshi Kanisawa, Hiroshi Yamaguchi, and Yoshiji Horikoshi
NTT Basic Research Laboratories, 3-1 Wakamiya, Morinosato, Atsugi, Kanagawa 243-01, Japan
(Received 6 May 1996)

The electronic properties of monolayer steps on $(2\times4)/c(2\times8)$ reconstructed GaAs(001) surfaces are measured using ultrahigh vacuum scanning tunneling microscopy. We propose unit structures for steps and demonstrate that steps play the role of acceptor arrays. An electron-counting consideration on the steps explains the densities of kinks in the As dimer rows on vicinal surfaces. We found that the acceptors at the steps are identical to those at the kinks. We confirmed that the surface states related to surface Fermi-level pinning are located at breaking points of a coherent arrangement of semiconducting (2×4) unit cells. [S0163-1829(96)05932-2]

Clarifying the microscopic relationship between surface atomic configurations and their electronic properties is essential in establishing surface physics and developing device technology, since it dominates both surface and interface macroscopic properties. The properties of $(2\times4)/c(2\times8)$ reconstructed GaAs(001) surfaces are particularly important because these surfaces are widely used to grow compound semiconductors or metal-semiconductor contacts by molecular-beam epitaxy (MBE). On the surface, depletion layer formation by surface Fermi-level pinning is a crucial phenomenon in improving device performance. To date, many different mechanisms for the phenomenon have been proposed,[1] but no mechanism has been conclusively explained to our knowledge. Recently, Pashley and Haberern reported a mechanism in which each kink in the dimer vacancy rows of $(2\times4)/c(2\times8)$ reconstruction acts as a single acceptor type trap. They suggested that the kink, one of the surface defects, formed to exactly compensate for space charges in the surface depletion region.[2] Further experiments by scanning tunneling spectroscopy and voltage-dependent scanning tunneling microscope (STM) imaging have shown that the kink plays the role of a surface acceptor, and the Fermi level is pinned at midgap.[3,4] In this paper, we clarify the relation between the atomistic structures of monolayer steps, the other surface defects, and their electronic properties on $(2\times4)/c(2\times8)$ reconstructed GaAs(001) surfaces. Although monolayer steps on the surface have been expected to be acceptor type surface traps,[2–5] atomistic study has not yet been undertaken. For this purpose, we have applied the electron counting model to ultrahigh vacuum scanning tunneling microscopy (UHV-STM) results of kink density on vicinal Si-doped GaAs(001) surfaces. The electron counting model requires that all dangling bond states of the electronegative element (As) will be filled by the available electrons in the surface layer, leaving all dangling bond states of the electropositive element (Ga) empty. If this condition is satisfied in a surface structure, the properties of the structure are semiconducting; otherwise they are metallic.[6] The metallic structure is expected to make surface states. Such an electron counting consideration has advantages in the qualitative analysis of surface chemical properties.

STM measurements were carried out in a UHV-STM system, which was combined with an MBE growth system. Vicinal GaAs surfaces were prepared by growing 2-μm-thick Si-doped GaAs layers at 570 °C on misoriented undoped GaAs(001) substrates that had been cut 0.5°, 1°, or 2° off (001) toward the $[111]A$ ($[\bar{1}\bar{1}\bar{1}]B$) crystal direction. The exactly oriented GaAs(001) substrate was also mounted on the same sample holder to allow kink density differences to be measured precisely. Si concentrations of 4×10^{18} and 2×10^{19} cm^{-3} were calibrated by secondary ion mass spectrometry. These Si concentrations were chosen so that surface kinks equaled or exceeded the number of unit cells at the steps on used vicinal surfaces. All doped Si atoms in the depletion layer are donors at these Si concentrations, and the surface electron densities are the same as those for kinks on exactly oriented surfaces.[2] Thus, these donor concentrations make the electronic effect on monolayer steps observable. Grown sample surfaces were protected from contamination[7] by an As passivation layer, and samples were transferred to an MBE chamber combined with UHV STM through air. As-protective layers were removed by annealing at temperatures up to 570 °C in As flux to obtain a satisfactory (2×4) structure, and to reproduce a (2×4) reconstructed reflection high-energy electron diffraction (RHEED) pattern. Then, the sample was quickly cooled down to room temperature, maintaining the (2×4) RHEED pattern. STM observation was performed at a bias voltage of -3.5 V and a tunneling current of 0.06 nA.

The high-resolution filled-state STM image in Fig. 1 shows the (2×4) surface of a 2-μm-thick exactly oriented GaAs(001) layer doped with Si at 4×10^{18} cm^{-3}. The dark lines along the $[1\bar{1}0]$ direction are dimer vacancy rows, and the dotted rectangular area indicates Chadi's $(2\times4)\beta2$ unit structure for two As dimers with dimer vacancy that is one monolayer below in height.[8] The (2×4) reconstructed area coexists with the $c(2\times8)$ area on a surface. The difference between the two areas arises from the arrangement of (2×4) unit cells relative to one another along the $[1\bar{1}0]$ direction. Thus, the relative atom arrangement around the kinks in As dimer rows in the (2×4) area (arrow A) is the same as that of the $c(2\times8)$ area (arrow B), and both kinks are expected to be equivalent single acceptor type surface traps.[2] A unit area with a kink (kink area) should have an integer ratio to that of a (2×4) unit cell. This is because

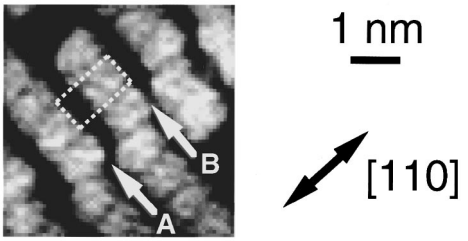

FIG. 1. High resolution filled-state STM image of kinks in As dimer vacancy rows. The area is 4.7 nm ×4.7 nm. Arrow *A* indicates a kink in the (2×4) reconstructed area and arrow *B* indicates a kink in the $c(2\times8)$ reconstructed area. Dotted rectangle shows a $(2\times4)\beta2$ unit cell.

kinks distribute at the boundary between semiconducting $(2\times4)/c(2\times8)$ reconstructed surfaces, which consist of coherently arranged (2×4) unit cells. Therefore, lateral potential periodicity along the $[1\bar{1}0]$ direction on the surface is expected to terminate symmetrically at the kink, namely, the surface state site, except for the existence of the additional dangling bond.

In Fig. 2, filled-state STM images of exactly oriented and vicinal GaAs(001) surfaces are shown. The doped Si concentration is 4×10^{18} cm^{-3}, and the misorientation angle is 1° for Figs. 2(b) and 2(c). The observed (2×4) unit structure is a $(2\times4)\beta2$ structure. Kink densities are 6.3×10^{12} cm^{-2} for exactly oriented surfaces (*J* surfaces), 2.3×10^{12} cm^{-2} for vicinal surfaces 1° off (001) toward $[111]A$, and 1.0×10^{12} cm^{-2} for vicinal surfaces 1°a off (001) toward $[111]B$, respectively. The kink density of the *J* surface is higher than those of vicinal surfaces. We also found that the kink density of the *A*-off surface is always higher than that of the *B*-offsurface at the same misorientation angle, and larger misori-entation angle induces lower kink densities.

To explain the misorientation-dependent kink density difference in STM results, we observed high resolution filled-state STM images at *A*-off steps and *B*-off steps [Figs. 3(a) and 3(b)] and determined the atomistic structures of steps for application to electron counting consideration. In Figs. 3(a) and 3(b), derived unit structure models of the $[111]A$ step and $[111]B$ step were superimposed on STM images. The atomistic configuration for the $(2\times4)\beta2$ unit structure is known as shown in Fig. 3, and each boundary of the (2×4) $\beta2$ structures on the surfaces is resolved in both Figs. 3(a) and 3(b). Therefore, by maintaining relative As dimer positions between layers the same as those in the unit structure, there is no other option in atomistic configuration at steps. Here, we ignored excessive sticking As molecule clusters on the surfaces. Each broken rectangular area indicates the unit structure for each step. The unit structure of the $[111]A$ step in Fig. 3(a) has a deficiency of 0.5 electron. There is no difference between the $[111]A$ step in the (2×4) reconstructed area and that in the $c(2\times8)$ reconstructed area. This is because the difference occurs as a result of the parallel shift of the (2×4) unit cells along the $[111]A$ steps. On the other hand, there are two types of unit structures for the $[111]B$ step as shown in Fig. 3(b). Type I is a typically observed $[111]B$ step structure and has a deficiency of 3 electrons per unit. Type II is an occasionally observed structure and is not deficient in electrons. The difference between type I and type II arises from the difference between the neighboring reconstruction areas at the $[111]B$ step. If the neighbors are of the same reconstruction area, consisting of either (2×4) or $c(2\times8)$ reconstruction, the unit structure can only be type I. However, if the neighbors are different from one another, i.e., one is (2×4) and the other is $c(2\times8)$, both type I and type II exist at the steps. Therefore, from the electron counting consideration, both

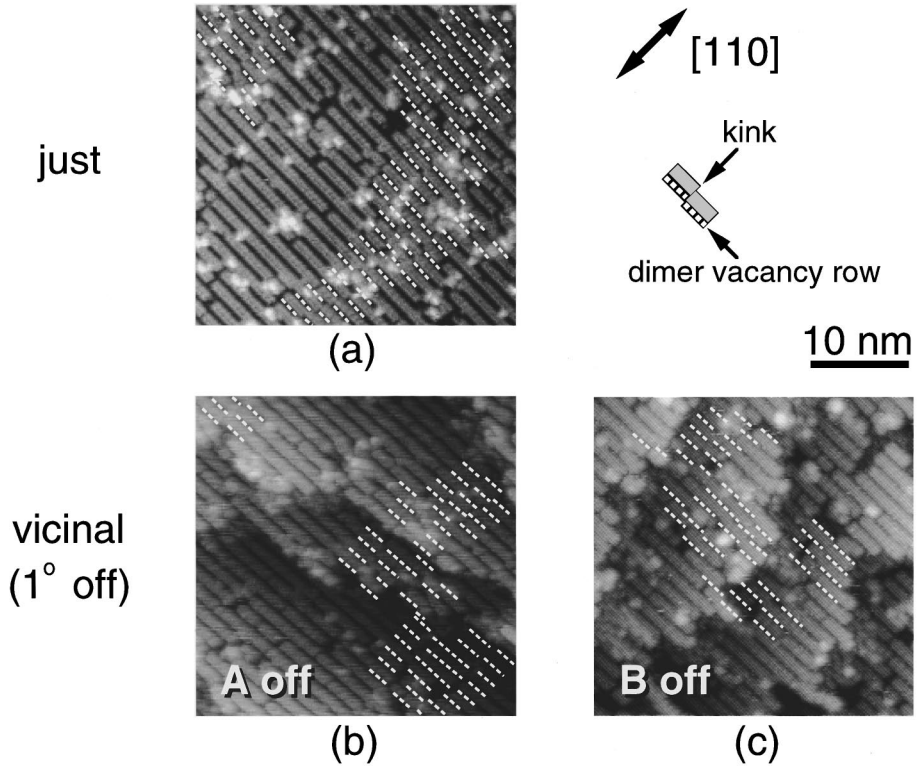

FIG. 2. Filled-state STM images of GaAs(001) surfaces. Each area is 33 nm×33 nm. (a) Exactly oriented (001), (b) 1° off (001) toward $[111]A$, and (c) 1° off (001) toward $[111]B$. Each broken line indicates As dimer vacancy row around kink.

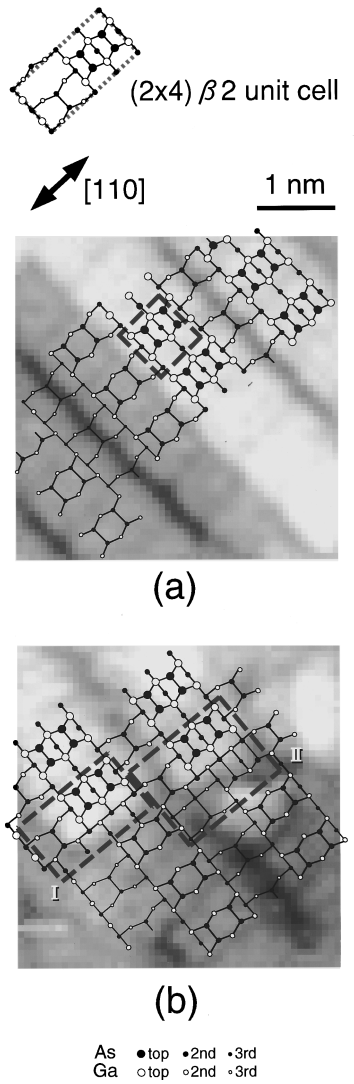

FIG. 3. High resolution filled-state STM images of steps with structure models superimposed. Each area is 4.4 nm×4.4 nm. Broken squares show unit structures of steps. (a) [111]*A* step. (b) [111] *B* step. The inset shows the structure of the $(2\times4)\beta2$ unit cell.

[111]*A* steps and [111]*B* steps are expected to play the role of acceptor arrays, and the arrays are expected to have a deficit of 0.5 electron for the [111]*A* step unit and a deficit of 3 or fewer electrons for the [111]*B* step unit. It should be noted that, from the noninteger ratios of all unit areas of [111]*A* and [111]*B* steps to that of a (2×4) unit cell, lateral potential periodicity along the [110] or [$1\bar{1}0$] direction on surfaces is expected to terminate asymmetrically at the steps. This condition is quite different from that of kinks in As dimer rows, and it indicates the possibility that acceptor type surface states by steps are different from those by kinks. Details will be provided later.

The kink density difference between the *J* surface and misoriented (001) surfaces of $\theta°$ off toward [111]*A* and [111]*B* (θA surface and θB surface) is shown in Fig. 4 to clarify the effects of acceptor type traps at steps and misorientation directions. The differences allow us to measure the effect of steps precisely by canceling other minor effects of surface defects such as missing (2×4) unit cells on terraces.

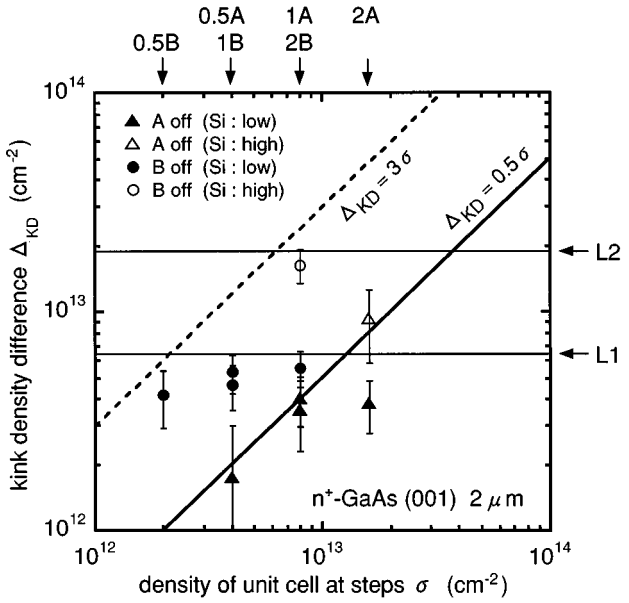

FIG. 4. Kink density difference between exactly oriented surface and vicinal surface, measured from STM images, as a function of density of unit cell at steps. $L1$ and $L2$ indicate densities of electrons from space-charge regions of Si concentration 4×10^{18} cm^{-3} (Si:low) and 2×10^{19} cm^{-3} (Si:high), respectively. Solid (broken) line shows results of electron counting consideration at steps for θA (θB) surface.

We plotted two data points in the case of a misorientation angle of 1° for each misorientation direction to confirm experimental accuracy. All of these data showed distributions within standard deviations (error bars in Fig. 4) of the statistical counting of kinks. The *x* axis indicates density of unit cells at steps and the corresponding misorientation conditions are shown at the top of the figure. Horizontal lines $L1$ and $L2$ indicate the densities of surface electrons from the space-charge regions of corresponding donor concentrations 4×10^{18} and 2×10^{19} cm^{-3}, respectively. We have also plotted the relations between unit structure densities and acceptor densities at steps derived from the former electron counting consideration using a solid line (*A*-off) and a broken line (*B*-off). With a Si concentration of 4×10^{18} cm^{-3}, kink density differences increase with increases in misorientation angles. Measured differences for the *A*-off (*B*-off) vicinal surface are distributed close to the solid (broken) line from the electron counting consideration at lower step densities and these finally converge to the $L1$ line. We also plotted differences at a higher Si concentration of 2×10^{19} cm^{-3} in Fig. 4. Complete STM results show good agreement with results from the electron counting consideration on proposed step structures. Furthermore, we performed STM measurement on surfaces with step bunching and found that a lower step density surface area has a higher density in kinks. We also found that the sum of kink density and that of the acceptor sites at steps is constant for each area on the same sample surface. From these results, we found two electronic features of steps. The first is that acceptors at steps play roles exactly equivalent to those at kinks in dimer rows, though the symmetries of surface potential periodicity terminations are different from each other. The second is that acceptor

type trap density on the surface is unquestionably dominated by electrons from space-charge regions depending only on donor concentration in layers, if space-charge density is sufficiently higher than step density. The donor concentration dependence of the kink density on exactly oriented GaAs(001) surfaces has been reported to be consistent with that of the surface state, which pins the surface Fermi level at the midgap.[9] These features suggest that surface Fermi level pinning is governed by these surface acceptors induced by structures disturbing the coherency of the semiconducting (2×4) unit-cell arrangement at the steps and the kinks. Therefore, we confirmed the surface Fermi level pinning mechanism by Pashley and Haberern.[2] Moreover, there was remarkable evidence that is related to the electronic properties of GaAs(001) surfaces. Although the symmetries of potential periodicity terminations are an intrinsic factor in the properties of surface states, both asymmetrical terminations at steps and symmetrical terminations at kinks are closely related to each other and result in the equivalent behavior of surface acceptors on the GaAs(001) surface. This suggests that local electron deficiency on surface unit structures is superior to the horizontal irregularity of the periodic surface potential for surface state properties on this surface. This is the principal reason for the applicability of the electron counting model in explaining the static surface properties of III-V compound semiconductors.

In conclusion, we performed UHV-STM measurements to clarify the relation between the atomistic structures and electronic properties on $(2\times4)/c(2\times8)$ reconstructed GaAs(001) surfaces. We proposed atomistic unit structures for the [111]*A* step and [111]*B* step on GaAs(001) surfaces based on high resolution STM images. Electron counting consideration on the proposed structures suggests that steps play the role of acceptor arrays, and this was confirmed by UHV-STM measurement on the vicinal surface. Experimental results show that acceptors at steps have equivalent properties to acceptors at kinks. We found that surface acceptor site densities are dominated by the density of surface electrons from the space-charge region to exactly compensate surface states, if surface electron density is substantially higher than step density. It was confirmed that surface Fermi-level pinning is a result of electron capture by the surface acceptor state through structures that disturb the coherency of semiconducting (2×4) unit cell arrangement at the steps and the kinks in As dimer rows.

We would like to thank Dr. Kenji Shiraishi for his helpful discussion on electron counting considerations and on the structural stability of surface atomic arrangement.

[1] R. H. Williams, Surf. Sci. **251/252**, 12 (1991).
[2] M. D. Pashley and K. W. Haberern, Phys. Rev. Lett. **67**, 2697 (1991).
[3] M. D. Pashley, K. W. Haberern, and R. M. Feenstra, J. Vac. Sci. Technol. B **10**, 1874 (1992).
[4] M. D. Pashley, K. W. Haberern, R. M. Feenstra, and P. D. Kirchner, Phys. Rev. B **48**, 4612 (1993).
[5] S. Chang, L. J. Brillson, Y. J. Kime, D. S. Rioux, P. D. Kirchner, G. D. Pettit, and J. M. Woodall, Phys. Rev. Lett. **64**, 2551 (1990).
[6] M. D. Pashley, Phys. Rev. B **40**, 10 481 (1989).
[7] S. K. Kowalczyk, D. L. Miller, J. R. Waldrop, P. G. Newman, and R. W. Grant, J. Vac. Sci. Technol. **19**, 255 (1981).
[8] D. J. Chadi, J. Vac. Sci Technol. A **5**, 834 (1987).
[9] H. Yamaguchi and Y. Horikoshi, Phys. Rev. B **53**, 4565 (1996).